Supporting Information:

Size-Dependent Band-Gap and Molar Absorption Coefficients of Colloidal $CuInS_2$ Quantum Dots

*Chenghui Xia,[a, b] Weiwei Wu,[a] Ting Yu,[a] Xiaobin Xie,[c] Christina van Oversteeg,[a] Hans C. Gerritsen[b] and Celso de Mello Donega[a]**

a. Condensed Matter and Interfaces, Debye Institute for Nanomaterials Science, Utrecht University, 3508 TA Utrecht, The Netherlands

b. Molecular Biophysics, Debye Institute for Nanomaterials Science, Utrecht University, 3508 TA Utrecht, The Netherlands

c. Soft Condensed Matter, Debye Institute for Nanomaterials Science, Utrecht University, Princetonplein 5, 3584 CC Utrecht, The Netherlands

*Corresponding author: E-mail: c.demello-donega@uu.nl

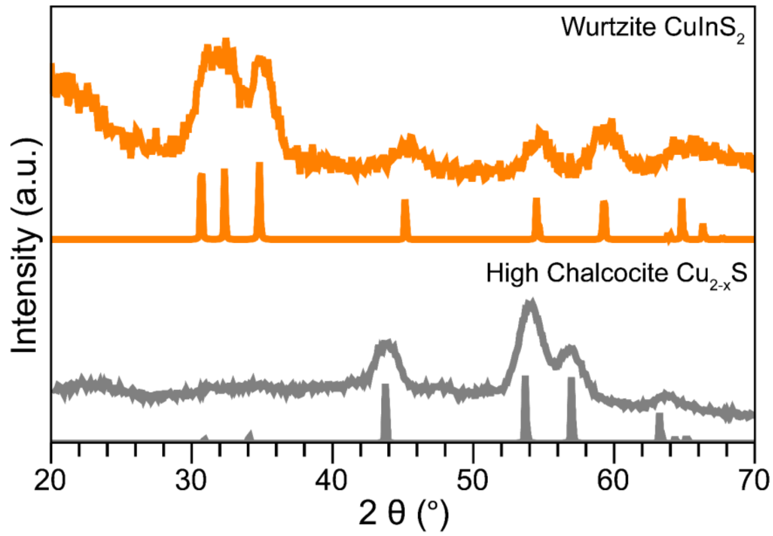

Figure S1. X-ray diffraction (XRD) patterns of template $Cu_{2-x}S$ NCs and product CIS QDs. The gray lines indicate the high-chalcocite Cu_2S diffraction pattern (JCPDS Card 00−026−1116). The orange lines indicate the wurtzite (wz) $CuInS_2$ diffraction pattern (JCPDS Card 01−077−9459). The XRD patterns were obtained on Bruker D2 Phaser, equipped with a Co Kα X-ray source (1.79026 Å).

Table S1. Detailed parameters for synthesizing wz CIS QDs *via* partial Cu^+ for In^{3+} cation exchange in different sizes of $Cu_{2-x}S$ NCs.

	Solution B			Solution A			Reaction Condition	
Sample	$Cu_{2-x}S$	DDT	ODE	$In(Ac)_3$	TOP	ODE	Temperature	Time
1	2.6 nm	0.5 ml	1.5 ml	0.0584 g	100 μl	2 ml	125 °C	90 min
2	3.2 nm	0.5 ml	1.5 ml	0.0584 g	100 μl	2 ml	125 °C	90 min
3	3.5 nm	0.5 ml	1.5 ml	0.0584 g	100 μl	2 ml	125 °C	100 min
4	4.2 nm	0.5 ml	1.5 ml	0.0584 g	100 μl	2 ml	125 °C	100 min
5	4.8 nm	0.5 ml	1.5 ml	0.0584 g	100 μl	2 ml	125 °C	110 min
6	5.2 nm	0.5 ml	1.5 ml	0.0584 g	100 μl	2 ml	125 °C	110 min
7	5.5 nm	0.5 ml	1.5 ml	0.0584 g	100 μl	2 ml	125 °C	120 min
8	5.9 nm	0.5 ml	1.5 ml	0.0584 g	100 μl	2 ml	125 °C	120 min
9	6.1 nm	0.5 ml	1.5 ml	0.0584 g	100 μl	2 ml	125 °C	130 min
10	6.2 nm	0.5 ml	1.5 ml	0.0584 g	100 μl	2 ml	125 °C	130 min
11	6.3 nm	0.5 ml	1.5 ml	0.0584 g	100 μl	2 ml	125 °C	140 min
12	6.9 nm	0.5 ml	1.5 ml	0.0584 g	100 μl	2 ml	125 °C	140 min
13	7.2 nm	0.5 ml	1.5 ml	0.0584 g	100 μl	2 ml	125 °C	150 min
14	7.4 nm	0.5 ml	1.5 ml	0.0584 g	100 μl	2 ml	125 °C	150 min

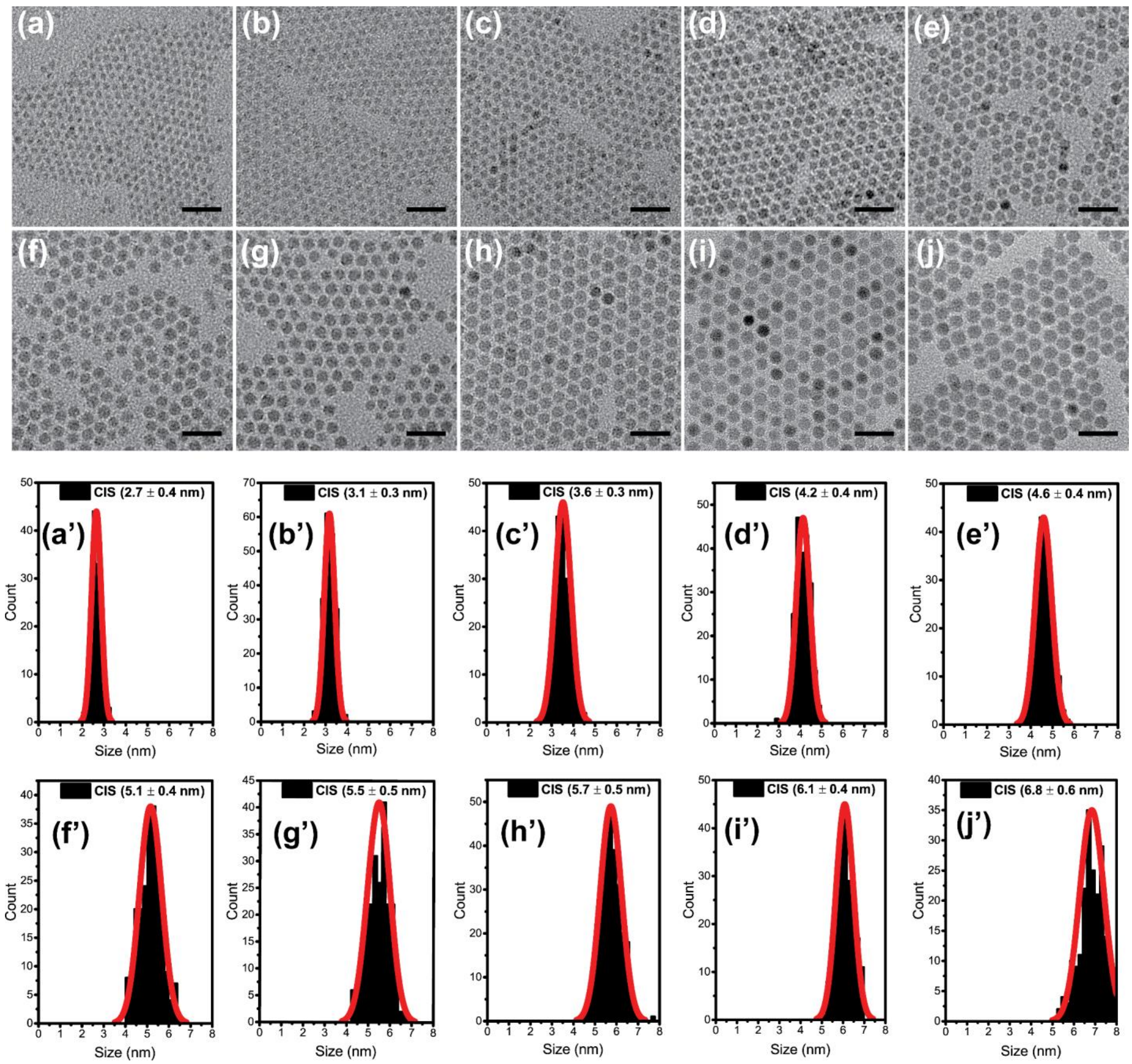

Figure S2. TEM images **(a-j)** and corresponding size histograms **(a'-j')** of CIS QDs with size ranging from 2.7 to 6.8 nm. The CIS QDs (polydispersity ≤10%) were obtained by topotactic partial Cu^+ for In^{3+} cation exchange in template $Cu_{2-x}S$ NCs. The size distribution histograms were constructed by measuring over 200 particles per image and were then fitted by a Gaussian distribution function. The scale bars are 20 nm.

Supporting Method 1: QD concentration (6.1 nm CIS QDs as an example).

From ICP measurements, the Cu^+ and In^{3+} concentration in product 6.1 nm CIS QDs are 0.00687 mmol/ml and 0.00576 mmol/ml, respectively. The product CIS QDs are wurtzite structure. In this hexagonal close packing, each unit cell possesses 2 cations (Cu^+ or In^{3+}) and 2 anions (S^{2-}). For simplicity, we approximate the Cu/In to 1. If the QD concentration is determined by Cu^+, then the QD concentration is deduced as follows:

As the average diameter (*d*) of the CIS QDs is 6.1 nm, the volume of a single QD is:

$$V_{QD} = \frac{4}{3}\pi(\frac{d}{2})^3 = \frac{4}{3}\pi(\frac{6.1}{2})^3 = 118.847\ nm^3 = 1.188 \times 10^5 Å^3$$

The unit cell volume of wurtzite CIS QDs is:

$$V_{uc} = a^2 c \cdot \sin 60^{\circ} = \frac{\sqrt{3}}{2} a^2 c = 84.99\ Å^3$$

The number of unit cells per QD is:

$$N_{unit/QD} = \frac{V_{QD}}{V_{uc}} = \frac{1.188 \times 10^5 Å^3}{84.99\ Å^3} = 1397.81$$

The number of Cu atoms in each unit cell is:

$$N_{Cu^+/uc} = 2 \times 50\% = 1$$

The number of Cu atoms per QD is:

$$N_{Cu^+/QD} = N_{unit/QD} \times N_{Cu^+/uc} = 1397.81$$

Since the Cu^+ amount of 1ml of product QDs is:

$$n_{Cu^+} = 0.00687\ mmol$$

The amount of QDs in 1 ml solution is:

$$n_{QDs} = \frac{N_A n_{Cu^+}}{N_A N_{Cu^+/QD}} = \frac{0.00687\ mmol}{1397.81} = 4.92 \times 10^{-6} mmol$$

Therefore, the CIS QDs concentration is 4.92×10^{-6} mmol/ml.

Table S2. Detailed parameters for synthesizing CIS QDs *via* partial Cu^+ for In^{3+} cation exchange in the 5.5 nm template $Cu_{2-x}S$ NCs.

	Solution B			Solution A			Reaction Condition	
Sample	$Cu_{2-x}S$ NO.	DDT	ODE	$In(Ac)_3$	TOP	ODE	Temperature	Time
1	5.5 nm	0.5 ml	1.5 ml	0.0584 g	100 µl	2 ml	125 °C	20 min
2	5.5 nm	0.5 ml	1.5 ml	0.0584 g	100 µl	2 ml	125 °C	40 min
3	5.5 nm	0.5 ml	1.5 ml	0.1168 g	200 µl	2 ml	125 °C	60 min
4	5.5 nm	0.5 ml	1.5 ml	0.1168 g	200 µl	2 ml	125 °C	80 min
5	5.5 nm	0.5 ml	1.5 ml	0.1752 g	300 µl	2 ml	125 °C	100 min
6	5.5 nm	0.5 ml	1.5 ml	0.1752 g	300 µl	2 ml	125 °C	120 min
7	5.5 nm	0.5 ml	1.5 ml	0.2336 g	400 µl	2 ml	125 °C	140 min
8	5.5 nm	0.5 ml	1.5 ml	0.2336 g	400 µl	2 ml	125 °C	160 min
9	5.5 nm	0.5 ml	1.5 ml	0.2920 g	500 µl	2 ml	125 °C	180 min
10	5.5 nm	0.5 ml	1.5 ml	0.2920 g	500 µl	2 ml	125 °C	200 min

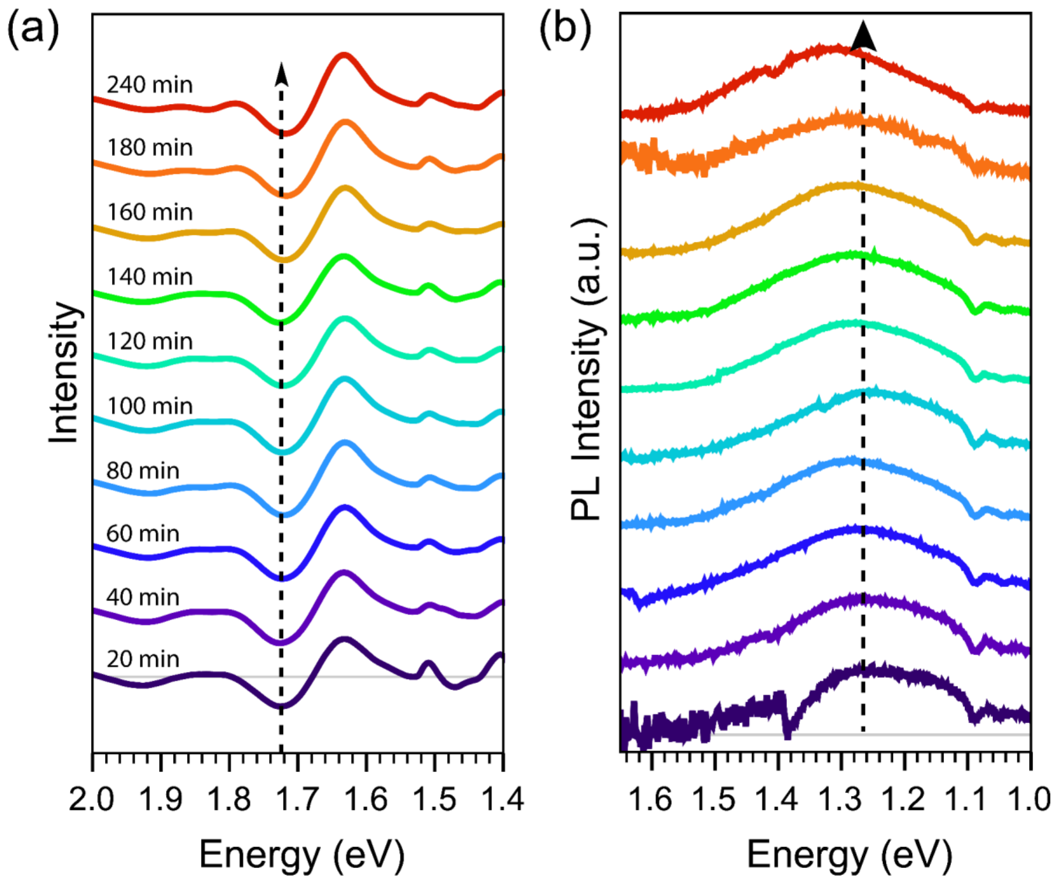

Figure S3. (a) Second derivative of the absorption spectra and **(b)** PL spectra of 5.5 nm wz CIS QDs. Ten different cation exchange reactions were performed using the same batch of 5.5 nm $Cu_{2-x}S$ NCs as templates and varying the reaction time (20–200 min) and the In/Cu feeding ratio (1 to 5), while keeping all other parameters constant (see Table S2 above for details). The dashed arrow lines indicate the increase of reaction time. All samples were measured under the same conditions (same QD concentration in trichloroethylene, excitation wavelength at 650 nm with a 715 nm long pass filter).

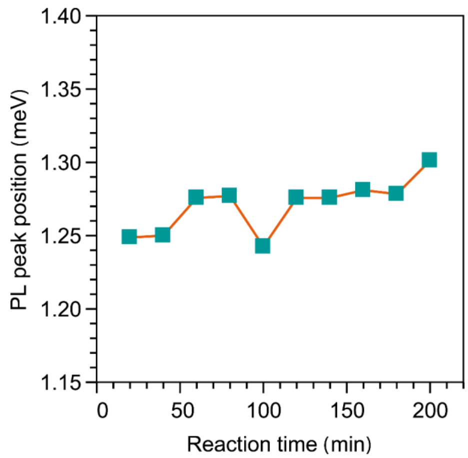

Figure S4. PL peak positions of different batches of 5.5 nm wz CIS QDs produced by partial Cu^{+} for In^{3+} cation exchange using the same batch of 5.5 nm $Cu_{2-x}S$ NCs as templates, and varying the reaction time (20–200 min) and the In/Cu feeding ratio (1 to 5), while keeping all other parameters constant (see Table S2 above for details).

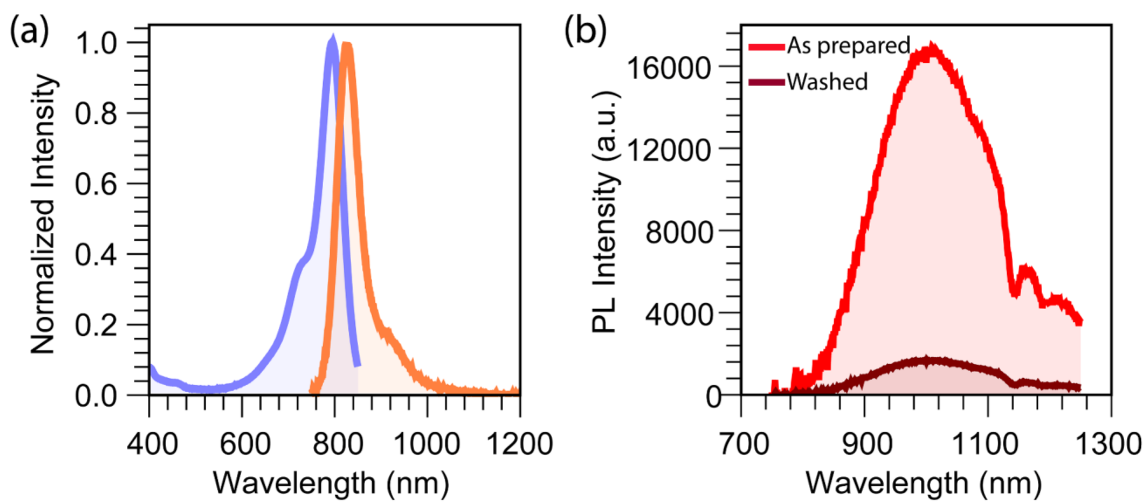

Figure S5. (a) Absorption (purple line) and PL (orange line) spectra of indocyanine green (ICG) in DMSO. This dye has a photoluminescence quantum yield (PLQY) of 12% in DMSO, and was used as a standard to determine the PLQYs of the product CIS QDs (see Methods in the main text for details). **(b)** PL spectra of 5.5 nm wz CIS QDs prior to (red line, PLQY~11%) and after 5 washing cycles (brown line, PLQY~1%).

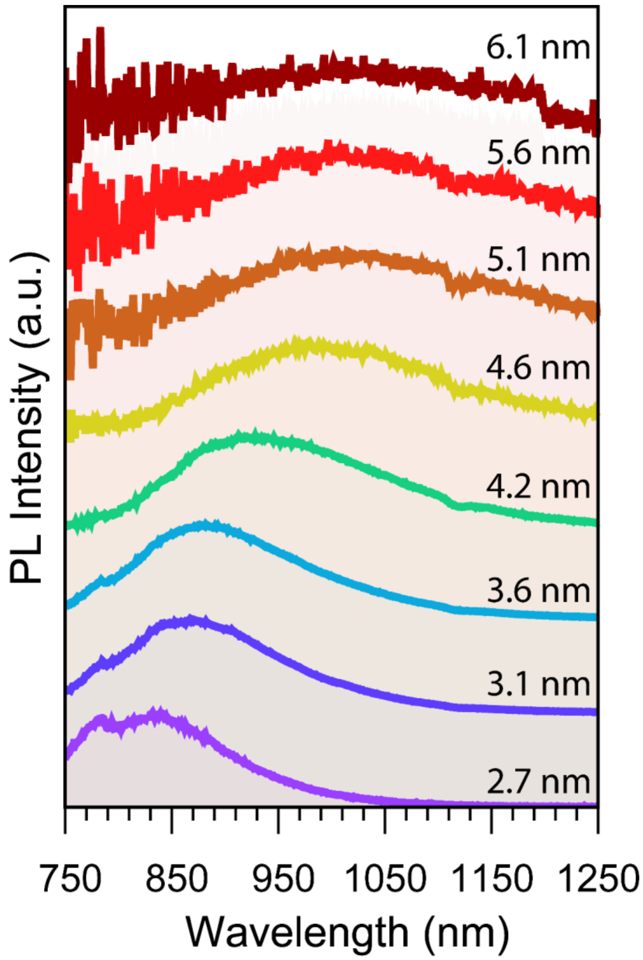

Figure S6. PL spectra of wz CIS QDs ranging from 2.7 to 6.1 nm in size. The spectra were corrected for the instrumental response. PL peak positions shift to longer wavelengths with increasing QD size. As the PL quantum yields of larger QDs are very low, the noise at the edge of detector (~750 nm) become obvious after correction for the instrumental response. All samples were measured under the same conditions (same QD concentration in trichloroethylene, Excitation wavelength at 650 nm with a 715 nm long pass filter).

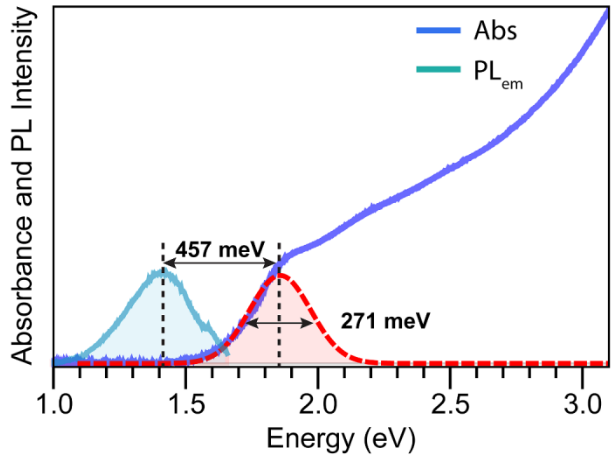

Figure S7. Absorption (blue solid line) and PL (cyan solid line) spectra of 3.6 nm wz CIS QDs. The dashed red line is the first absorption peak obtained by fitting a Gaussian distribution function centered at the lowest absorption transition energy, which is determined from the second derivative of the absorption spectrum.

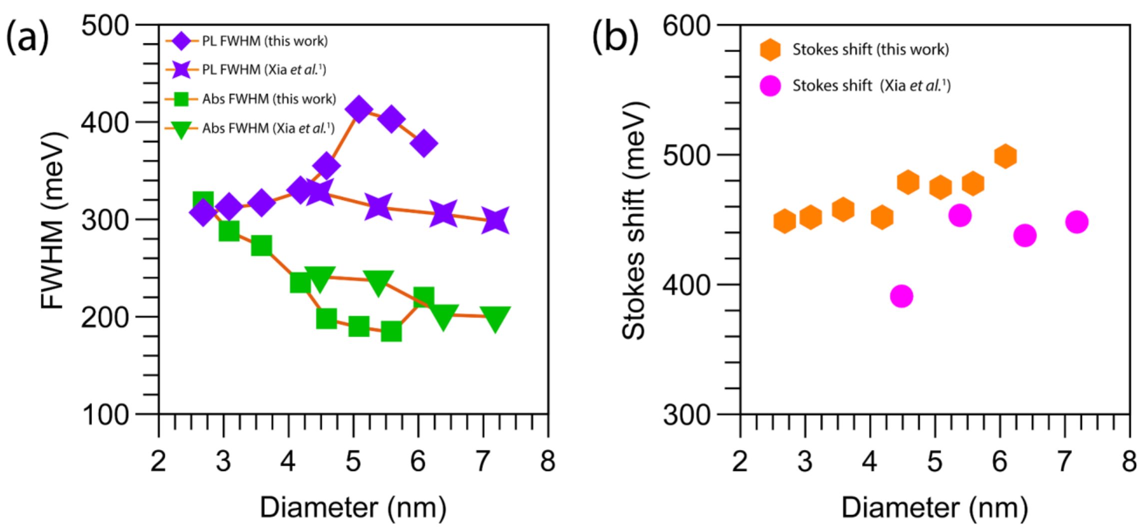

Figure S8. (a) Full-width at half-maximum (FWHM) of the lowest energy absorption transition (Abs, green symbols) and of the PL band (PL, purple symbols) of wz CIS QDs prepared in the present work (squares, In/Cu= 0.91±0.11, PLQY≤1%) and reported in our previous work [1] (triangles and stars, In/Cu= 0.7±0.1, PLQY from 22% to 3.4% in the 5.4 to 7.2 nm size range). The FWHM of lowest energy absorption transition is obtained as shown in Figure S7 above. The PL FWHM is obtained by fitting a Gaussian distribution function to the PL spectrum in energy scale. It should be noted that the PL FWHM of the samples with diameters larger than 4.2 nm are less reliable due to the higher signal to noise ratio of their PL spectra (see Figure S6 above). **(b)** Global Stokes shifts of the wz CIS QDs investigated in the present work (hexagons) and in our previous work [1] as a function of their diameter.

Table S3. In/Cu feeding and actual ratios of CIS QD samples used in previous studies to obtain the data shown in Figure 4b. ICP= Inductively Coupled Plasma Spectroscopy; EDX: Energy Dispersive X-Ray Spectroscopy; XPS= X-ray Photoelectron Spectroscopy.

Reference	**Feeding amount of In and Cu precursors**	**In/Cu ratio in the product CIS QDs**
Qin *et al.* [2]	0.1 mmol $In(acetate)_3$ + 0.1 mmol CuCl (In/Cu=1)	Product NCs are reported to be nearly stoichiometric (by EDX), but the actual ratio and EDX data are not provided
Booth *et al.* [3]	0.25 mmol $In(acetate)_3$ + 0.25 mmol CuI (In/Cu=1)	In/Cu= 1 (by EDX) and 0.91 (by XPS)
Zhong *et al.* [4]	1.0 mmol $In(acetate)_3$ + 1.0 mmol CuI (In/Cu=1)	The composition is size dependent: 3.6 nm (In/Cu= 0.58 by EDX and 0.42 by ICP) 4.0 nm (In/Cu= 0.64 by EDX and 0.50 by ICP) 5.1 nm (In/Cu= 0.74 by EDX and 0.56 by ICP) 5.5 nm (In/Cu= 0.83 by EDX and 0.56 by ICP) 6.1 nm (In/Cu= 0.97 by EDX and 0.58 by ICP) 7.6 nm (In/Cu= 1.09 by EDX and 0.88 by ICP)
Li *et al.* [5]	1.0 mmol $In(acetate)_3$ + 1.0 mmol CuI (In/Cu=1)	The composition is size dependent: 2.2 nm (In/Cu= 1.04 by EDX) 2.7 nm (In/Cu= 1.03 by EDX) 3.3 nm (In/Cu= 0.93 by EDX)
Berends *et al.* [6]	1.0 mmol $In(acetate)_3$ + 1.0 mmol CuI (In/Cu=1)	Not reported
Akdas *et al.* [7]	0.66 mmol $In(acetate)_3$ + 0.66 mmol Cu(I) acetate (In/Cu=1)	In/Cu= 1.1 by ICP

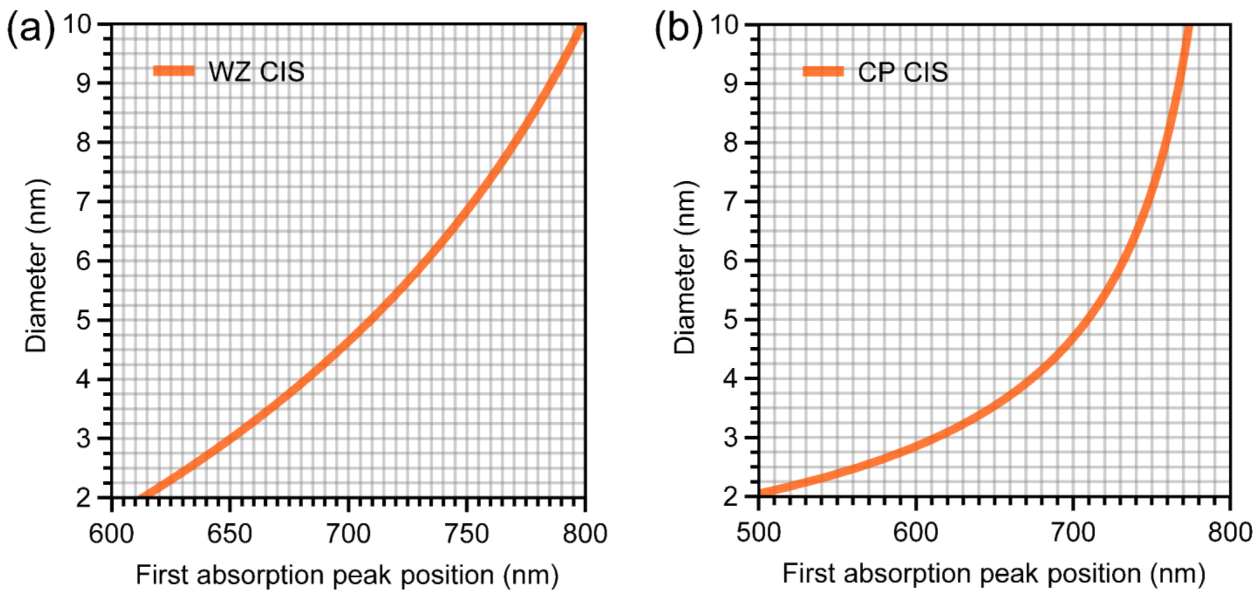

Figure S9. Sizing curves of wz **(a)** and cp **(b)** CIS QDs. The curves are obtained from fits to experimental data reported in Figure 4 in the main text (equations 3 and 4).

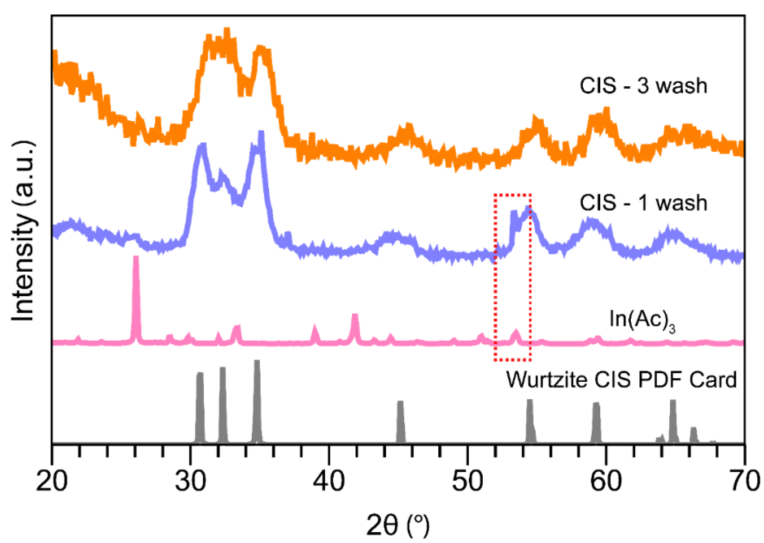

Figure S10. XRD patterns of CIS QDs washed once (blue) or three times (orange). The gray line indicates the wurtzite CIS diffraction pattern (JCPDS Card 01−077−9459). The pink line is the XRD pattern of $In(Ac)_3$ (99.99%). The dashed red box indicates that the additional peak in the CIS QDs that were washed only once may originate from residual $In(Ac)_3$. After 3 washing cycles, no additional peak can be detected, which implies complete removal of unreacted indium salts. The XRD patterns were obtained on Bruker D2 Phaser, equipped with a Co Kα X-ray source (1.79026 Å).

REFERENCES

1. Xia, C.; Meeldijk, J. D.; Gerritsen, H. C.; de Mello Donegá, C. Highly Luminescent Water-Dispersible NIR-Emitting Wurtzite $CuInS_2$/ZnS Core/Shell Colloidal Quantum Dots. *Chem. Mater.* **2017**, *29*, 4940–4951.
2. Qin, L.; Li, D.; Zhang, Z.; Wang, K.; Ding, H.; Xie, R.; Yang, W. The Determination of Extinction Coefficient of $CuInS_2$, and $ZnCuInS_3$ Multinary Nanocrystals. *Nanoscale* **2012**, *4*, 6360–6364.
3. Booth, M.; Brown, A. P.; Evans, S. D.; Critchley, K. Determining the Concentration of $CuInS_2$ Quantum Dots from the Size-Dependent Molar Extinction Coefficient. *Chem. Mater.* **2012**, *24*, 2064–2070.
4. Zhong, H.; Lo, S. S.; Mirkovic, T.; Li, Y.; Ding, Y.; Li, Y.; Scholes, G. D. Noninjection Gram-Scale Synthesis of Monodisperse Pyramidal $CuInS_2$ Nanocrystals and Their Size-Dependent Properties. *ACS Nano* **2010**, *4*, 5253–5262.
5. Li, L.; Pandey, A.; Werder, D. J.; Khanal, B. P.; Pietryga, J. M.; Klimov, V. I. Efficient Synthesis of Highly Luminescent Copper Indium Sulfide-Based Core/Shell Nanocrystals with Surprisingly Long-Lived Emission. *J. Am. Chem. Soc.* **2011**, *133*, 1176–1179.
6. Berends, A. C.; Rabouw, F. T.; Spoor, F. C. M.; Bladt, E.; Grozema, F. C.; Houtepen, A. J.; Siebbeles, L. D. A.; de Mello Donegá, C. Radiative and Nonradiative Recombination in $CuInS_2$ Nanocrystals and $CuInS_2$-Based Core/Shell Nanocrystals. *J. Phys. Chem. Lett.* **2016**, *7*, 3503–3509.
7. Akdas, T.; Walter, J.; Segets, D.; Distaso, M.; Winter, B.; Birajdar, B.; Spiecker, E.; Peukert, W. Investigation of the Size-Property Relationship in $CuInS_2$ Quantum Dots. *Nanoscale* **2015**, *7*, 18105–18118.